ISBN: 978-3-95450-233-2 ISSN: 2673-5504 doi:10.18429/JACoW-SRF2021-MOPTEV006

SYNCHROTRON XPS STUDY OF NIOBIUM TREATED WITH NITROGEN INFUSION*

A. Prudnikava†, Y. Tamashevich, O. Kugeler, J. Knobloch, HZB, Berlin, Germany
S. Babenkov[1], V. Aristov, O. Molodtsova, DESY, Hamburg, Germany
D. Smirnov, Technical University of Dresden, Dresden, Germany
A. Makarova, Free University of Berlin, Berlin, Germany
[1]presently at CEA-Saclay, Paris, France

Abstract

Processing of niobium cavities with the so-called nitrogen infusion treatment demonstrates the improvement of efficiency and no degradation of maximal accelerating gradients. However, the chemical composition of the niobium surface and especially the role of nitrogen gas in this treatment has been the topic of many debates. While our study of the infused niobium using synchrotron X-ray Photoelectron Spectroscopy (XPS) showed modification of the surface sub-oxides surprisingly there was no evidence of nitrogen concentration build up during the 120°C baking step, irrespectively of N_2 supply. Noteworthy, that the niobium contamination with carbon and nitrogen took place during a prolonged high-temperature anneal even in a high vacuum condition (10^{-8}-10^{-9} mbar). Evidently, the amount of such contamination appears to play a key role in the final cavity performance

INTRODUCTION

Vacuum thermal processing is a key technological step in the cavity production technology. It has been established that a low-temperature baking at 120°C/48 h eliminates a so-called Q_0-slope and provides more stable accelerating gradients [1]. In the last years new treatments, nitrogen doping [2] and infusion [3], have been elaborated. The $Q_0(E_{acc})$ curve demonstrated anti-Q slope which has not been previously observed. With these treatments improving of the efficiency up to three times and moderate maximal accelerating fields is possible to obtain.

Evidently, the increased interstitial content in the near-surface Nb region upon such treatments is leading to coupled effects associated with the modulation of electron mean free path and "dirty superconductivity" [4], suppression of hydride formation by hydrogen trapping [5] and as a consequence a reduction of residual resistance. In order to find a possible origin of anti-Q slope, determine a role of nitrogen supply in the chamber during the low-temperature baking step and further optimize the Nb surface treatment procedure extensive studies of chemical composition and crystal structure are required. Here we are exploring the "classic" infusion recipe by synchrotron radiation XPS using small Nb samples, study the effect of N_2 supply during 120°C baking step, and explore the Nb surface in a high vacuum environment immediately after the high-temperature anneal step.

EXPERIMENTAL DETAILS

The samples were cut by electro-erosion from 2.8 mm-thick large-grain Nb sheets (Heraeus) followed by buffered chemical polishing (BCP), water and ethanol rinsing. The annealing experiments were performed in a furnace consisting of a ceramic tubular chamber (7 cm in diameter, 1.5 m in length) with a three-zone temperature control providing a base pressure of 10^{-6} mbar at 800°C. The titanium polycrystalline tubular holder covered with Nb foil was used both as a getter material and a sample support. Several treatments were tested on samples. Here we present the results on the 800°C vacuum anneal (800°C/2–$3\cdot10^{-6}$ mbar/3h), nitrogen infusion (800°/3h + 120°C/$4\cdot10^{-2}$ mbar of N_2/48h), and infusion without N_2 supply (800°/3h, 2-$3\cdot10^{-6}$ mbar + 120°C/$7.5\cdot10^{-7}$ mbar/48h). After the treatment, the samples were subjected to ambient atmosphere for a couple of days and transferred to XPS set up for further investigation. The samples are compared to the same large-grain Nb chemically pre-treated in a same way but thermally annealed in high-vacuum (800-950°C/$2\cdot10^{-8}$ – $2.5\cdot10^{-9}$ mbar/11h) in the preparation chamber of the XPS set-up. The sample was studied immediately after the annealing upon cooling to room temperature in ultra-high vacuum (without air exposure).

Investigation of the chemical composition of the first set of samples was performed using synchrotron radiation XPS at the end-station based on Argus analyzer with the 128-channel high sensitive detector and integrated to P04 beamline, PETRAIII. Several photon energies (PEs) of the incident beam in the range of 800-1500 eV and at an angle close to normal emission (72°) were used. The latter sample was measured at dipole RGBL, BESSYII synchrotron radiation facility (HZB, Berlin) at PE 450-1000eV, normal emission geometry at 55° angle between the incident beam and an analyzer aperture. The binding energies were calibrated using Au $4f_{7/2}$ core level peak from a metal foil. Nb 3d, Nb 3p, O 1s, C 1s, N 1s, and in some cases Ti 2p core-level spectra have been analysed using the CasaXPS software package. The samples were additionally characterized by SEM, XRD (Bruker D8 Advance, Cu kα), and Raman spectroscopy (MonoVista SP-2500i, 532 nm DPSS-laser, 5 mW).

* Work supported by INNOVEEA program within the Helmholtz Gemeinschaft
† alena.prudnikava@helmholtz-berlin.de

ISBN: 978-3-95450-233-2 ISSN: 2673-5504 doi:10.18429/JACoW-SRF2021-MOPTEV006

RESULTS AND DISCUSSION

All the samples were inspected with SEM but no morphological changes (precipitates of new phases) were observed. The XRD measurements were performed in two geometries. Bragg-Brentano and grazing incidence. In Bragg-Brentano geometry the XRD pattern contains mainly a reflection from the niobium surface plane (200) normal to the scattering vector (Fig. 1a). Also, low-intensity peaks from (101), and (211) crystal planes are visible owing to the surface roughness provided with BCP.

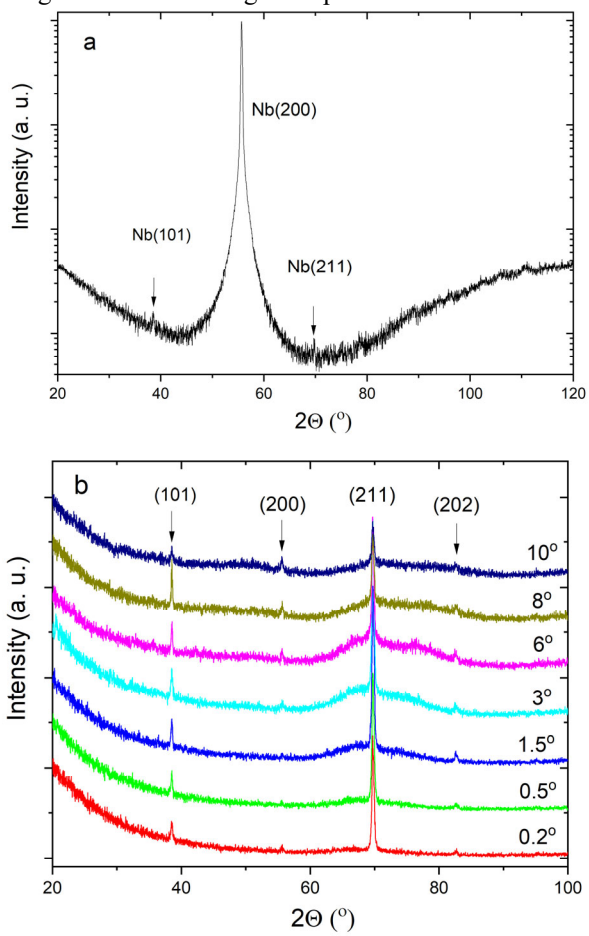

Figure 1: XRD patterns of the infused sample measured in Bragg-Brentano (a) and grazing incidence (b) geometry.

In order to gain more surface information, the XRD was also measured in grazing-incidence geometry at various incidence angles (ω=0.2 – 8°). However, only the peaks characterizing niobium were detected (Fig. 1b).

Raman spectra (Fig. 2) taken from all the samples looked very similar, and contained weak peaks at the following stretching frequencies: 140, 150, 170, 270, 308, 485, 548, 564, 670, and 850 cm^{-1}, that were reported for Nb-O modes of vibration in the [NbO_6] octahedra as well as among the octahedra in various polymorphs of Nb_2O_5 [6]. No stretching modes corresponding to nitrides or carbides were observed.

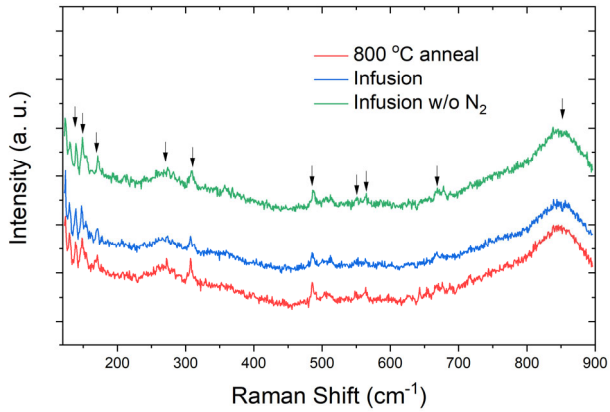

Figure 2: Raman Spectra of the niobium subjected to various processing recipes (λ=532 nm).

In Fig. 3, the XPS survey spectra of Nb samples processed with the three basic recipes are presented. The main peaks characterizing the surface state are pronounced. The spectra look similar and are dominated by Nb 3d, O 1s, C 1s, and N 1s core level transitions. O KLL Auger feature is also visible. The niobium subjected to infusion recipe contains a distinct Ti 2p feature, unlike the other treatments. From this result we may conclude that nitrogen flow in the vacuum chamber during 120°C baking step promotes surface contamination of the treated metal with titanium originating from the sample holder in our set-up. Evidently, the Ti vapor is created in the chamber during the preceding 800°C-step. The approximate Ti content within the information depth (i.e. the maximal depth normal to the surface from which 90% percent of the signal originates) of 4.4 nm was estimated to be 2.3 at%, along with Nb(22%), O(52.6%), C(22%), N(3.2%). By analyzing Ti 2p region (not shown) it was revealed that titanium is in the oxidation states Ti^{+4} and Ti^{+2}, corresponding to TiO_2 (88%) and Ti_2O_3(12%).

The core-levels of interest collected at high resolution for the infused sample are shown in Fig. 4(a-d). The spectra collected at 1200 eV of incident photons are shown as an example, and represent the background-subtracted experimental data with fitted components.

The N 1s has very low intensity and characterized by a broad peak at above 400 eV (Fig. 4a) originating from the organic nitrogen-containing species adsorbed at the surface inhomogeneities after handling it in ambient environment. A broad feature at 396.6 eV was observed at 1000-1200 eV photon energies but not at 800 eV. We assume that part of it (at 397 eV centroid maximum) may originate from a small amount of nitrogen bonded to niobium.

ISBN: 978-3-95450-233-2 ISSN: 2673-5504 doi:10.18429/JACoW-SRF2021-MOPTEV006

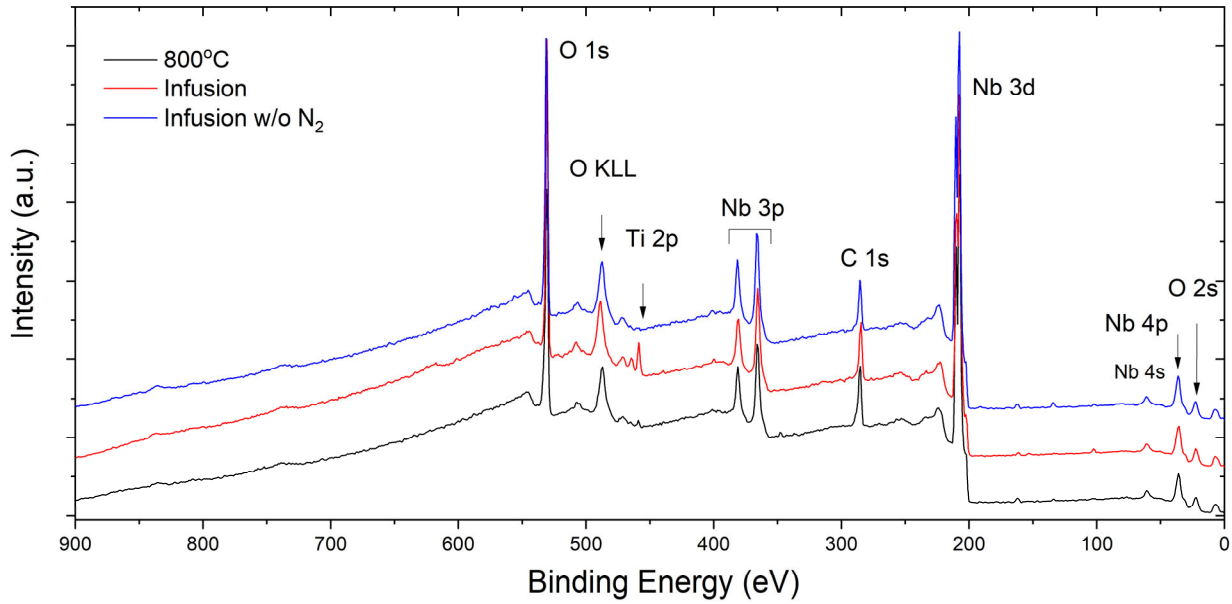

Figure 3: Wide-range XPS survey spectra the 800°C-annealed, N-infused and infused w/o N_2 Nb(100) samples collected at PE 1000 eV.

Since this region was not clearly resolved, and also the presence nitrides was not revealed by other techniques, the Nb nitride phases were not considered in the fitting model of Nb 3d of the first set of samples.

C 1s core level is represented by carbonaceous adsorbate commonly found at the surfaces of solids after the exposure to air atmosphere which is often called adventitious carbon. (Fig. 4b). Thus, no carbide phases were found in the experimental conditions under investigation.

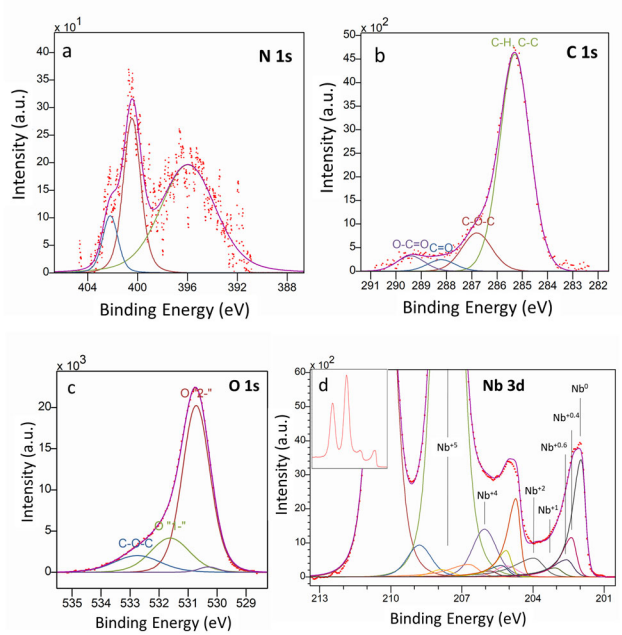

Figure 4: Background-subtracted XPS spectra of the N-infused niobium (PE=1200 eV): N 1s (a), C1s (b), O 1s (c), Nb 3d (d). Inset: unprocessed Nb 3d spectrum.

O 1s was fitted with three contributions (Fig. 4c) associated with O^{-2} ions in niobium oxides (530.6 eV), low coordinated O^{-1} ions that are compensating for some deficiencies in the oxide subsurface [7], and a peak at 532.7 eV that may be referred to weakly adsorbed species such as aliphatic C-O-C, etc [8].

A fourth component at 530.2 eV was added to account for Ti oxides present in this sample.

For the designation of Nb state, the core level peak features were decomposed as doublets with a constant spin orbital splitting of 2.75 eV and branching ratio $3d_{5/2}/3d_{3/2}$ of 1.5. The Nb 3d spectra were fitted with seven doublets corresponding to pure Nb and niobium oxides with the oxidation states ranging from +5 to +1. Contributions from oxygen interstitials in octahedral positions of niobium crystal lattice were also included in the model as $Nb^{+0.6}$ and $Nb^{+0.4}$. Peak positions, as well as their FWHMs are summarized in Table 1. The Nb 3d spectrum with the fitted components of the N-infused sample is presented in Fig. 4d as an example. The relative percentage areas of the fitted Nb 3d region for the three types of treatment are summarized in Table 2. Non-significant differences in some components were found, i.e. the 800°C-sample has the smallest percentage of Nb^{+5} as compared to the both infused samples. The calculated thickness of Nb_2O_5 layer is 3.5 nm vs 3.8 nm for the annealed and infused niobium, respectively. Also, the infused Nb has appeared to have the smallest amount of Nb^{+4} and Nb^{+2}. As to the interstitials content, they were equal for both the 800°C- and infused samples, while minimal for the infused w/o N_2 sample.

To gain more information about the interstitial phases, a new niobium sample was thermally annealed in high vacuum at 950°C/11h and was studied by XPS without intermediate air exposure (Fig. 5a-d). The as-treated Nb surface has appeared to be free from surface adsorbates and a top pentoxide layer which significantly attenuate the

ISBN: 978-3-95450-233-2 ISSN: 2673-5504 doi:10.18429/JACoW-SRF2021-MOPTEV006

Table 1: The FWHMs and Binding Energies and of the Nb Compounds Obtained by Fitting of the Photoemission Spectra

Oxidation state	Nb^{+5}	Nb^{+4}	Nb^{+3}	Nb^{+2}	Nb^{+1}	$Nb^{+0.6}$	$Nb^{+0.4}$	Nb
BE shift, eV	5.66±0.01	4.13±0.11	3.14±0.09	1.99±0.05	1.08±0.03	0.64±0.04	0.39±0.03	0
FWHM, eV	1.16±0.07	1.18±0.16	1.13±0.09	1.03±0.26	0.76±0.06	0.66±0.10	0.53±0.11	0.44±0.07

Table 2: Relative Area of the Fitted Components of Nb 3d Core Level of the Annealed, Infused, and Infused Without Nitrogen Niobium

PE, eV	Nb^{+5}	Nb^{+4}	Nb^{+3}	Nb^{+2}	Nb^{+1}	$Nb^{+0.6}$	$Nb^{+0.4}$	Nb
800°C	70.31±0.19	6.94±0.14	1.11±0.23	4.18±0.16	1.07±0.18	1.51±0.09	3.28±0.08	11.61±0.15
Infusion	75.44±0.17	5.29±0.09	1.32±0.20	3.51±0.18	1.43±0.13	1.49±0.06	3.27±0.06	8.26±0.11
Infusion w/o N_2	72.49±0.17	7.39±0.20	0.90±0.18	4.63±0.39	1.68±0.14	0.56±0.09	2.94±0.08	9.41±0.13

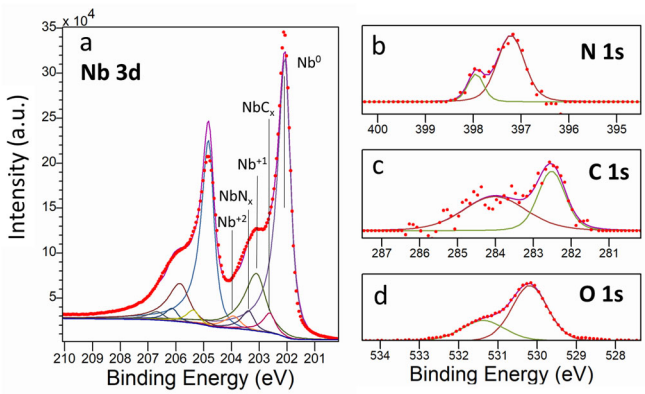

Figure 5: XPS spectra of niobium (221) annealed at 950°C (PE=480 eV): Nb 3d (a), N 1s (b), C 1s (c), and O 1s taken at PE 650 eV (d).

photoelectrons from beneath. Nb oxides normally present at the niobium surface in ambient environment were reduced, and the peaks corresponding to Nb^0 and Nb^{+1} and Nb^{+2} evidently Nb_2O and NbO, were detected within Nb 3d.

O 1s was featured by the oxygen bound to Nb with peaks at 530.2 (O^{-2}) and 531.4 eV (O^{-1}). Apart from that, Nb reacted with nitrogen and carbon. N 1s despite its low intensity is complex, i.e. has at least two components (397.2 and 398 eV) testifying the formation of Nb-N and Nb-N-O bonds. The peak at 282.5 eV of niobium carbide was only detected at a low PE providing a high surface sensitivity (information depth 1.8 nm at PE 480 eV). Residual gas analyzer registered approximately $6.7 \cdot 10^{-10}$ mbar of CO, $1.0 \cdot 10^{-9}$ mbar of CO_2 and $1.4 \cdot 10^{-9}$ mbar of H_2O at 300°C and total base pressure of $1.3 \cdot 10^{-8}$ mbar, and $1.6 \cdot 10^{-9}$ of N_2 and the same of CO, $1.6 \cdot 10^{-10}$ of CO_2, $4.6 \cdot 10^{-10}$ mbar of H_2O in the chamber at 885°C and total base pressure of $1.9 \cdot 10^{-8}$ mbar. At 955°C at the end of anneal only H_2O ($1.3 \cdot 10^{-10}$ mbar) and CO ($2.7 \cdot 10^{-10}$ mbar) were detected in the chamber at total base pressure of $2.5 \cdot 10^{-9}$ mbar. Evidently, at a lower temperature (800°C) and a smaller duration of anneal (2-3h) the nitridation and carburization would be even more negligible (below the detection limit of XPS) in high vacuum condition. Thus, one should not consider a prolonged 800°C step as a route to receive a purer Nb surface - even if the residual gas pressure is extremely low. We may unambiguously claim that the niobium carbide and nitride precipitation occurs at 800°C in large furnaces for cavity anneal which typically provide a higher working base pressure (10^{-6}-10^{-8} mbar). The size, quantity and proportion of the two phases (along with Nb oxides) would be affected by the residual gas composition in the chamber, temperature ramp during the heating stage, and the initial surface state of niobium surface (proper surface chemical preparation and cleaning has to be provided). The presence of carbon in the system would affect the formation of various sub-oxide phases during the thermal treatment and also subsequently upon air exposure due to its reduction properties [9]. It is evident that excess amount of the three compounds (NbO_x, NbN_x, and NbC_x) would lead to cavity performance deterioration [10], since the formed phases are not superconducting at 2K in the present experimental conditions (at least according to the current state of knowledge), but their optimal content has to be further investigated as well as a particular effect of low-temperature baking step on these phases in the infusion recipe.

CONCLUSION

We have performed processing of Nb samples with the basic cavity treatment schemes: 800°C anneal, infusion and infusion without nitrogen gas. No carbide or nitride phases formation was detected upon any of the treatment in our experimental conditions after the exposure to air by SEM, XRD and synchrotron radiation XPS. The latter technique revealed a trace amount of titanium oxides at the surface of the infused sample with the conclusion that a continuous N_2 supply in the vacuum chamber may act as a

ISBN: 978-3-95450-233-2 ISSN: 2673-5504 doi:10.18429/JACoW-SRF2021-MOPTEV006

carrier of vaporised Ti from the sample holder. Mild-baking step was found to increase the Nb_2O_5 top oxide insignificantly (03-0.5 nm), while no effect of N_2 addition was detected onto Nb phase formation in our experiments.

Niobium after the 11h-anneal in high vacuum revealed the formation of negligible amount of niobium carbide and nitride phases (along with Nb_2O and a trace amount of NbO) in the niobium surface layer of few nanometers. This was only possible in the in-situ XPS experiment providing a clean Nb surface free from organic and gas adsorbates as well as the native Nb_2O_5. The amount of these phases most likely determines whether the infusion treatment would provide the gain or deterioration in the quality factor during the cavity operation.

ACKNOWLEDGEMENTS

We acknowledge the opportunity to perform measurements at the facilities of Helmholtz-Zentrum Berlin: the X-Ray CoreLab, especially A. Ramírez Caro, and Russian-German dipole beamline. We express special thanks to B. Rau and K. Mack for the access and assistance in performing Raman Spectroscopy investigation. A.M. and D.S. acknowledge the BMBF (grant no. 05K19KER and 0519ODR, respectively).

REFERENCES

[1] B. Visentin, "Improvement of Q-slope for high fields", in *Proc. R&D Issues in Superconducting Cavities (TESLA Meeting)*, Hamburg, Germany, p. 57, March 1998.

[2] A. Grassellino *et al.*, "Nitrogen and argon doping of niobium for superconducting radio frequency cavities: a pathway to highly efficient accelerating structures", *Supercond. Sci. Technol.,* vol. 26, no. 10, p. 102001, 2013. doi:10.1088/0953-2048/26/10/102001

[3] A. Grassellino *et al.*, "Unprecedented quality factors at accelerating gradients up to 45 MVm^{-1} in niobium superconducting resonators via low temperature nitrogen infusion", *Supercond. Sci. Technol.,* vol. 30, no. 9, p. 094004, 2017. doi:10.1088/1361-6668/aa7afe

[4] H. Padamsee, *RF Superconductivity: Science, Technology, and Applications*. John Wiley & Sons, 2009.

[5] G. Pfeiffer, and H. Wipf, "The trapping of hydrogen in niobium by nitrogen interstitials", *J. Phys. F: Met. Phys.,* vol. 6, no. 2, p. 167, 1976. doi:10.1088/0305-4608/6/2/013

[6] Bill X. Huang *et al.,* "Characterization of oxides on niobium by Raman and infrared spectroscopy", *Electrochim. Acta,* vol. 44, no. 15, pp. 2571-2577, 1999. doi:10.1016/S0013-4686(98)00385-5

[7] J.-Ch. Dupin *et al.*, "Systematic XPS studies of metal oxides, hydroxides and peroxides", *Phys. Chem. Chem. Phys.*, vol. 2, no. 6, pp.1319-1324, 2000. doi:10.1039/A908800H

[8] G. Beamson *et al.*, *High Resolution XPS of Organic Polymers - The Scienta ESCA300 Database*, Wiley Interscience, 1992, Appendices 3.1 and 3.2.

[9] K. Ono, "Physico-chemical aspects of the Nb-C-O system and production of niobium and its alloys by carbothermic reduction and electron beam melting", *High Temp. Mater. Processes*, vol. 11, no. 1-4, pp. 207-216, 1993. doi:10.1515/HTMP.1993.11.1-4.207

[10] M. Wenskat *et al*., "Nitrogen infusion R&D at DESY a case study on cavity cut-outs", *Supercond. Sci. Technol.,* vol. 33, no. 11, p. 115017, 2020. doi:10.1088/1361-6668/abb58c